Molecular Biotechnology
https://doi.org/10.1007/s12033-024-01185-8

ORIGINAL PAPER

Sophoraflavanone G Inhibits RANKL-Induced Osteoclastogenesis via MAPK/NF-κB Signaling Pathway

Xinchun Li[3,5,6,7] · Wei Deng[3,8,9] · Kai Tang[3,8,9] · Shiyin Zhang[3,8] · Zixuan Liang[3,8] · Weiwen Liu[3,8] · Yongyu Li[3,8] · Zhida Zhang[1] · Wenhua Zhao[4] · Jian Zou[2,3]

Received: 12 January 2024 / Accepted: 19 April 2024

Abstract

Osteoporosis is a common chronic bone metabolism disorder characterized by decreased bone mass and reduced bone density in the bone tissue. Osteoporosis can lead to increased fragility of the skeleton, making it prone to brittle fractures. Osteoclasts are macrophage-like cells derived from hematopoietic stem cells, and their excessive activity in bone resorption leads to lower bone formation than absorption during bone remodeling, which is one of the important factors inducing osteoporosis. Therefore, how to inhibit osteoclast formation and reducing bone loss is an important direction for treating osteoporosis. Sophoraflavanone G, derived from *Sophora flavescens Alt* and *Rhizoma Drynariae*, is a flavonoid compound with various biological activities. However, there have been few studies on osteoporosis and osteoclasts so far. Therefore, we hypothesize that genistein G can inhibit osteoclast differentiation, alleviate bone loss phenomenon, and conduct in *vitro* and in *vivo* experiments for research and verification purposes.

Keywords Sophoraflavanone G · Osteoporosis · Osteoclasts · *Sophora flavescens Alt* · *Rhizoma Drynariae*

Xinchun Li, Wei Deng and Kai Tang have been contributed equally to this work.

✉ Zhida Zhang
spinezzd@yeah.net

✉ Wenhua Zhao
13539961409@163.com

✉ Jian Zou
15812855286@163.com

1 Orthopedics Department, The Affiliated Traditional Chinese Medicine Hospital, Guangzhou Medical University, Guangzhou City 510405, Guangdong Province, China

2 Orthopedic Spine Department, Dongguan Hospital of Traditional Chinese Medicine, Dongguan City 523005, Guangdong Province, China

3 Guangzhou University of Chinese Medicine, Guangzhou City 510405, Guangdong Province, China

4 Orthopedics Department, The Second Affiliated Hospital of Guangzhou Medical University, Guangzhou City 510260, Guangdong Province, China

5 Department of Orthopaedic, Hainan Traditional Chinese Medicine Hospital, Hainan City, China

6 Department of Orthopaedic, Affiliated Hainan Traditional Chinese Medicine Hospital, Hainan City 570203, Hainan Province, China

7 Department of Orthopaedic, Affiliated Hainan Traditional Chinese Medicine, Hainan City 570203, Hainan Province, China

8 The Laboratory of Orthopaedics and Traumatology of Lingnan Medical Research Center, Guangzhou University of Chinese Medicine, Guangzhou City 510405, Guangdong Province, China

9 Orthopedics Department, The Affiliated TCM Hospital of Guangzhou Medical University, Guangzhou City 510405, Guangdong Province, China

Published online: 23 May 2024

Introduction

Osteoporosis (OP) is a chronic progressive systemic metabolic disease characterized by the reduction in bone mass and deterioration of bone microarchitecture, leading to increased bone fragility and resultant osteoporotic fractures [1, 2]. Primary OP is observed in postmenopausal women due to aging and in men aged over 70, while secondary OP often results from diseases, therapeutic methods, or specific factors including tumor formation, endocrine disorders, long-term use of glucocorticoids, unhealthy lifestyle habits, and severe depression [3, 4]. Globally, with the formation of an aging societal structure, by 2050, approximately a quarter of the population in major regions of the world, will either have reduced bone mass or be diagnosed with OP. This scenario will impose significant psychological and economic burdens on individuals, families, and society [5, 6].

Osteoclasts (OC), which originate from the mononuclear macrophage lineage and have bone resorption functions, are one of the key factors inducing OP. Their dynamic interaction with osteoblasts (OB), responsible for bone formation, together promotes skeletal growth and continuous bone remodeling. If this dynamic balance is disrupted by external or internal factors, it can lead to abnormal bone growth or relative or absolute active bone resorption, resulting in conditions such as bone hyperplasia, arthritis, osteogenesis imperfecta, and OP [7–9].

OC exhibits specificity during their formation and differentiation, especially in the process of fusing from mononuclear cells to multinucleated cells. The fusion and the multinucleation of OC are considered important characteristics of mature OC formation and bone resorption function. This process includes cell migration, identification, and cell fusion [10]. Precursor OC cells display specificity when choosing fusion ''partners''. This characteristic mainly depends on the stage of OC differentiation and the expression level of related fusion factors such as CD47 and Cx43 [11, 12].

OC has always been the direct target of many treatments aimed at preventing bone loss from various bone diseases, especially anti-bone resorption drugs like bisphosphonates (BP) and Denosumab, which have been very successful in treating OP and other diseases of bone loss. Long-term use of BP can significantly increase bone mineral density (BMD) and reduce the risk of vertebral fractures, improving survival rates. Even after discontinuation, they can still play a role in maintaining bone mass [13]. However, the concomitant use of BP is also associated with atypical femoral fractures, medication-related osteonecrosis of the jaw, gastrointestinal symptoms, and muscle pain, among other adverse reactions [14, 15]. Denosumab is a protein that targets the binding of RANK-RANKL, effectively inhibiting RANK activation through competitive binding with RANKL, portraying an inhibitory role. However, since RANKL is also expressed in immune cells such as T cells, Denosumab may potentially impact certain functions of the human immune system [16, 17]. Hence, the development of novel drugs aimed at inhibiting the bone resorption functions mediated by OC, managing bone remodeling, and treating OP, while simultaneously avoiding and reducing the adverse reactions of clinical medication, constitutes one of the prime topics of interest amongst current clinical researchers [18].

Sophoraflavanone G (SG, CAS: 97,938-30-2) is the flavonoid compound derived from *Sophora flavescens Alt* and *Rhizoma Drynariae*. Modern pharmacological studies have shown that it has various biological activities, such as anti-inflammatory, antioxidant, anti-tumor, and liver protection.SG inhibits tumor growth and promotes cell apoptosis induced by oxidative stress through the EGFR-PI3K-AKT signaling pathway. It can also specifically inhibit the expression of phosphorylated STAT and block the signaling of the NF-κB pathway, showing potential for cancer treatment [19, 20].

Due to its high bioavailability and significant immunomodulatory potential, SG can improve asthma symptoms by reducing airway inflammation-related oxidative stress [21, 22].SG can also reduce the release of inflammatory factors and neurotransmitters in the hippocampus system, block the signaling targets of rapamycin in mammals, and have an anti-depressive effect [23]. Modern biological studies have shown that SG can bind to the specific protein CTSK related to OC bone resorption function with high stability and interact with CTSK, inhibit the formation of bone resorption pits, and has the potential to inhibit OC differentiation and treat OP [24]. Based on its research progress and literature support, and the important role of OC in preventing and treating osteoporosis, we hypothesize that SG can inhibit OC cell differentiation and reduce bone loss.

Materials and Methods

Cell Preparation

Following the regulations of the Animal Ethics Committee of Guangzhou University of Traditional Chinese Medicine (Ethics Number: 20231009001), 6-week-old C57BL/6 J mice (provided by the San Yuan Li Experimental Animal Center of Guangzhou University of Traditional Chinese Medicine) were overdosed with 3% pentobarbital sodium at 40 ~ 45 mg/kg. Bilateral femurs and tibias were removed surgically, and transferred to α-MEM medium, excessive muscle tissue was removed, and bone marrow was flushed out under sterile conditions. After centrifuging at room temperature for 5 min at 1000 rpm, the supernatant was discarded, the sediment was resuspended in α-MEM complete medium (containing 10% FBS, 1% P/S, and 50 ng/mL M-CSF) and transferred to a T75 culture flask. The

medium was replaced every day until cells covered about 90% of the flask's bottom, and then the cells were digested, passaged, and subjected to the following experiments.

Reagents Preparation

Sophoraflavanone G (SG, CAS: 97,938-30-2) was purchased from Chamface Biotech Biotechnology Co., Ltd. (Wuhan, China) and dissolved in Dimethyl Sulfoxide (DMSO) to achieve a concentration of 100 mM and stored at − 80 °C for future use. MEM-α, (Cat #12,571,063), Fetal Bovine Serum (FBS, Cat #10099141C), Penicillin–Streptomycin Solution (P/S, Cat #15,140,122), and Parenzyme (Cat #25,200,056) were obtained from Thermo Fisher Scientific (China) Limited (Shanghai, China). Recombinant Mouse TRANCE/RANK L (Cat #: 462-TEC-010) and Recombinant Mouse M-CSF Protein (Cat #416-ML-050) were sourced from R&D Systems (Shanghai, China). DAPI(Cat #C0065), CCK-8 Cell Proliferation and Cytotoxicity Assay Kit(Cat #CA1210), Tartrate-resistant acid phosphatase (TRAP) Stain Kit (Solarbio, G1492) is sourced from Solarbio Technology Co., Ltd. (Beijing, China)0.2X SYBR Green Pro Taq HS Premix (Cat #AG11701) and Evo M-MLV RTase Enzyme Mix (Cat #AG11705) were purchased from Accurate Biology Biotechnology Co., Ltd. NFATc1 (Cat #DF6446), c-Fos (Cat #AF5354), MMP9 (Cat #AF5228), CTSK (Cat #DF6614), p38 MAPK (Cat #AF6456), Phospho-p38 MAPK (Thr180/Tyr182) (Cat #AF4001), ERK1/2 (Cat #AF0155), Phospho-ERK1/2 (Thr202/Tyr204) (Cat #AF1015), JNK1/2/3 (Cat #AF6318), Phospho-JNK1/2/3 (Thr183 + Tyr185) (Cat #AF3318), β-actin (Cat #AF7018) were all purchased from Affinity Biosciences Biotechnology Co., Ltd. (Jiang Su, China).

Cell Toxicity/Proliferation Assay

BMMs were seeded in 96-well plates at a density of 5 × 103 cells/well. The next day, different concentrations of SG (0 μM, 1 μM, 2 μM, 4 μM, 6 μM, 8 μM) were added and incubated for 48 h. Then, 10 μl of CCK-8 solution was added to each well and incubated in the dark for 2 h. The absorbance of each group was measured at 450 nm, and the bar chart was generated. The cell toxicity and proliferation effects of SG were statistically analyzed using GraphPad Prism 8 (v.8.0.2).

TRAcP Staining

BMMs were seeded in 96-well plates at the density of 5×10^3 cells/well. After the cells adhered, they were treated with RANKL (50 ng/mL), M-CSF (50 ng/mL), and different concentrations of SG (0 μM, 2 μM, 4 μM, 6 μM, 8 μM) to induce OC differentiation. Fresh medium was replaced every other day until mature OC formed on days 6–7. The medium was discarded, and the cells were fixed with 4% paraformaldehyde at room temperature for 10 min. And then stained according to the TRAcP kit instructions. Mature OC was observed and photographed under the inverted fluorescence microscope, with cells having ≥ 3 nuclei considered as mature OC.

Molecular Docking

Using the chemical name ''Sophoraflavanone G'' and CAS: 97,938-30-2, the TCMSP (https://tcmsp-e.com/) and PubChem (https://pubchem.ncbi.nlm.nih.gov/) databases were searched to obtain target information and structural formulas. Potential drug target information was obtained from the SwissTargetPrediction database (http://www.swisstargetprediction.ch/).

Intersection genes between SG drug targets and genes related to osteoporosis were further analyzed for their functions. The WebGestalt (https://www.webgestalt.org/) was used for GO enrichment analysis, dividing functions into three levels: biological processes, cellular components, and molecular functions. Additionally, the Metascape platform was used to create network maps to analyze the involved signaling pathways. SG was selected as the ligand, and its mol2 format small molecule 2D structure was downloaded from the TCMSP (https://tcmsp-e.com/). The corresponding protein structure in PDB format was downloaded from the RCSB PDB (https://www.rcsb.org/) database as the receptor. Molecular docking was conducted using AutoDock software (*v4.2*). The docking effects of key targets and active ingredients were assessed based on the affinity values. The higher the affinity, the better the binding activity between the ligand and receptor protein, and the more stable the docking state.

RT-PCR

Cells were seeded in 6-well plate at the density of 8 × 104 cells/well. During OC differentiation, cells were stimulated with RANKL (50 ng/mL), M-CSF (50 ng/mL), and varying concentrations of SG (0 μM, 4 μM, 8 μM). Total RNA was extracted using the TRIZOL method, and the obtained RNA was reverse transcribed to cDNA using the EVOM-MLV reagent kit. The PCR reaction was performed using the SYBR Green reagent kit. All related gene expression results were processed with the RT-PCR machine (Biorad, USA). The relative expression levels of each gene were calculated using the $2^{-\Delta\Delta CT}$ method. All primers are listed in Table 1 [25, 26].

Western Blot

BMMs were seeded in 6-well plate at the density of 8 × 104 cells/well. The next day, the cells were stimulated with RANKL (50 ng/mL), M-CSF (50 ng/mL), and varying concentrations of SG (0 μM, 8 μM) to induce OC differentiation.

Table 1 Primer List

Gene	Forward (5–3)	Reverse (5–3)	Tm (m3
NFATc1	GGAGAGTCCGAGAATCGAGAT	TTGCAGCTAGGAAGTACGTCT	60
c-Fos	GCGAGCAACTGAGAAGAC	TTGAAACCCGAGAACATC	60
CTSK	AGGGAAGCAAGC ACTGGATA	GCTGGCTGGAATCACATCTT	60
ACP5	CGTGTCTGGAGATTCGACTTGA	TTGGAAACTCACACGCCAGA	60
β-actin	GGCTGTATTCCCCTCCATCG	CCAGTTGGTAACAATGCCATGT	61

Table 2 Binding affinity results of Sophoraflavanone G with relevant target proteins

Compound	Target	Affinity (kcal/mol)
SophoraflavanoneG	ERK	− 8.7
SophoraflavanoneG	P38	− 7.3
SophoraflavanoneG	JNK	− 8.8
SophoraflavanoneG	IκB-α	− 6.4
SophoraflavanoneG	P65	− 6.8

After 6–7 days, the culture medium was discarded and cells were lysed on ice for 30 min using RIPA lysis buffer containing protease and phosphatase inhibitors. The protein lysate was then centrifuged at 15,000 g for 15 min at 4 °C. The protein concentration was determined using the BCA assay kit, and the molecular docking results with SG and the target protein are presented in Table 2.

Animal Experiment

By the ethical guidelines of Guangzhou University of Chinese Medicine's Animal Ethics Committee, animals were randomly divided into the following three groups: Sham surgery (Sham), OP model (OVX), and drug intervention (SG, 8 mg/kg). Mice were anesthetized with pentobarbital sodium at the standard dose of 40–45 mg/kg. Depending on the assigned group, different surgical procedures were performed. In the Sham group, only some fat near the ovaries was removed. In the OVX group, a bilateral oophorectomy was conducted. After surgery, the mice were closely monitored for 5–6 h until they fully recovered from anesthesia. Postoperative wound healing was monitored, and mice were given intraperitoneal injections at a standard dose of 8 mg/kg every other day.

Three months later, the mice were euthanized by CO_2 inhalation and their hind limbs were surgically removed and fixed in 4% paraformaldehyde for about 48 h. Afterwards, the limbs were soaked in 0.9% saline solution. Limbs were scanned using the Bruker SkyScan 1176 system at the resolution of 9 μM. The collected images were analyzed and reconstructed using CTAn (*v.1.10*) and DataViewer (*v.2.1*) software. Quantitative analysis was conducted on the trabecular bone region, including bone volume/tissue volume (BV/TV), trabecular number (Tb. N), trabecular thickness (Tb. Th), and trabecular separation (Tb. Sp).

Statistical Analysis

All results were meticulously scrutinized employing the GraphPad Prism 8.0 software, with the outcome data expressed via the $x \pm s$. The *t*-test was harnessed for juxtaposition between two data sets while a single-factor variance analysis was utilized for comparisons across multiple data sets. *P*-value less than 0.05 is designated to indicate statistical significance.

Results

SG Shows No Exhibit of Cytotoxic Influence

We evaluated the cytotoxic or proliferative effects of different concentration gradients of SG on BMMs under continuous stimulation for 48 h. Figure 1A displays the chemical structure of IGG, while the CCK-8 results (Fig. 1B) suggest that SG concentrations below 8 μM do not have significant cytotoxic or proliferative effects on BMM cells.

SG Inhibits OC Formation

To investigate whether SG could inhibit mature OC formation, we first stimulated BMMs with RANKL (50 ng/mL), M-CSF (50 ng/mL), and various SG concentrations (0 μM, 2 μM, 4 μM, 6 μM, 8 μM) to induce OC differentiation. Figure 1C, D show that SG significantly inhibits mature OC differentiation, and this inhibitory effect strengthens with increasing concentration, showcasing the clear concentration-dependent characteristic.

SG Suppresses Specific Gene Expression in Osteoclastogenesis

To determine the effects of SG on specific protein expression during OC differentiation, we used RT-PCR to assess the expression levels of CTSK, c-Fos, NFATc1, and MMP9. The results revealed that genes associated with OC differentiation

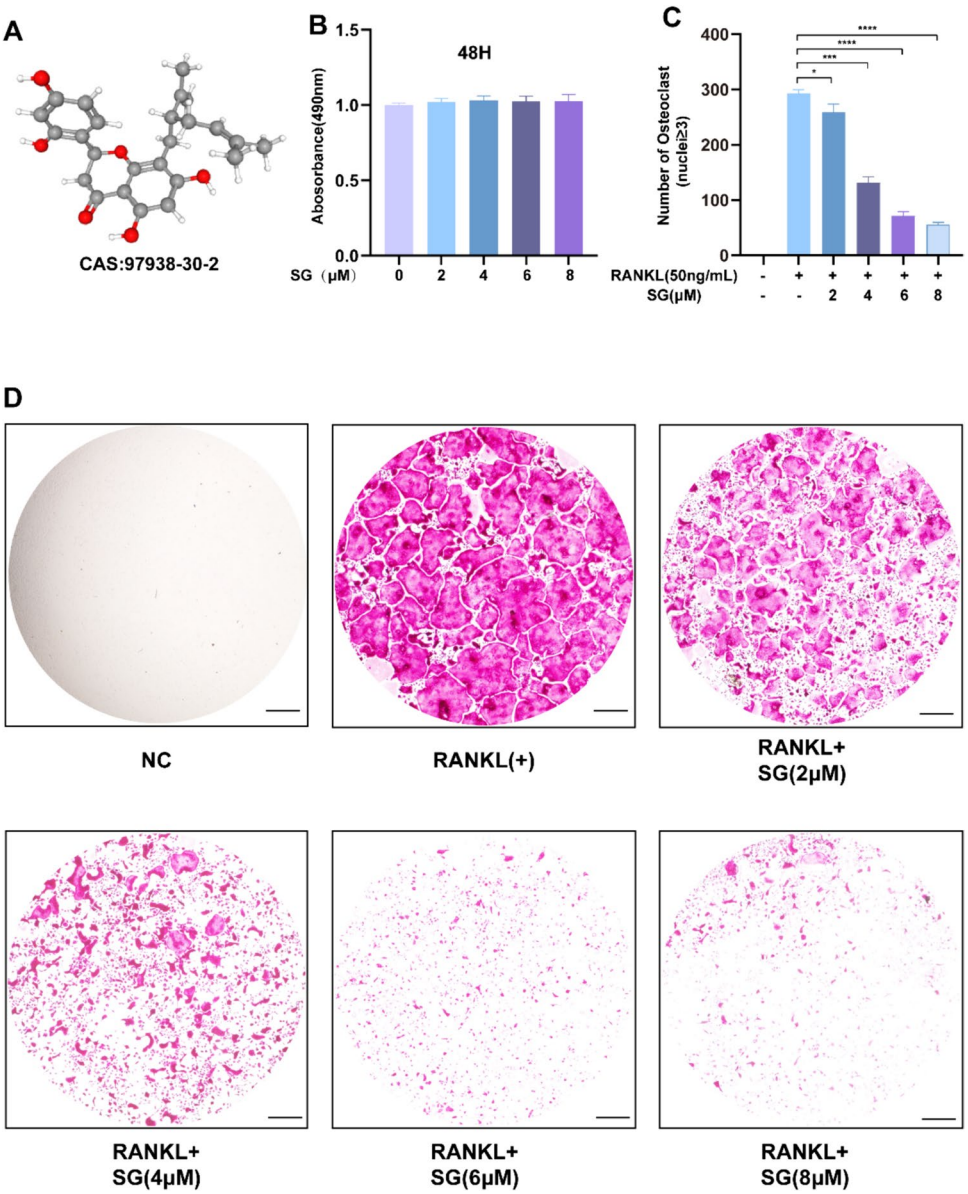

Fig. 1 Sophoraflavanone G (SG) can inhibit osteoclastogenesis. **A**: Chemical structure of SG; **B**: 48-h CCK-8 results demonstrate no cytotoxic or proliferative effects on BMMs when SG ≤ 8 μM; **C**: Different concentrations of SG show varying effects on RANKL-induced osteoclastogenesis, with higher concentrations exhibiting more pronounced inhibitory effects, demonstrating a clear concentration-dependent characteristic; **D**: Representative TRAcP staining images showing the inhibitory effects of various SG concentrations on OC differentiation. $*p < 0.05$, $**p < 0.01$, $***p < 0.001$ ($n = 3$). Scale bar = 200 μm

were substantially elevated under RANKL stimulation; however, under SG influence, all these genes displayed decreasing expression trends (Fig.2A, B, C, D).

SG Inhibits Protein Expression Specific to OC Differentiation

By extracting proteins at different time points, we studied the influence of SG on protein relative expression levels to explore its impact on OC differentiation. As shown in Fig. 2E, under RANKL stimulation, proteins MMP9, c-Fos, and NFATc1 showed a gradual increase on days 3 and 5. However, under SG's influence, all three exhibited suppressive trends, especially pronounced on day 5. CTSK reached its peak on day 3 and slightly decreased on day 5, but under SG stimulation, its expression was highest on day 3 and slightly lower on day 5. Figure 2F provides a bar chart analysis of the relative expression levels of proteins specific to OC differentiation.

GO and KEGG Analysis

Using network pharmacology, we explored the biological functions, signaling pathways, and binding affinities of specific proteins closely related to SG and OC differentiation. As shown in Fig. 3A, the GO analysis revealed biological and molecular functions closely associated with SG, such as the transmembrane receptor protein tyrosine kinase signaling pathway, protein autophosphorylation, positive regulation of kinase activity, ATP binding, and protein tyrosine kinase

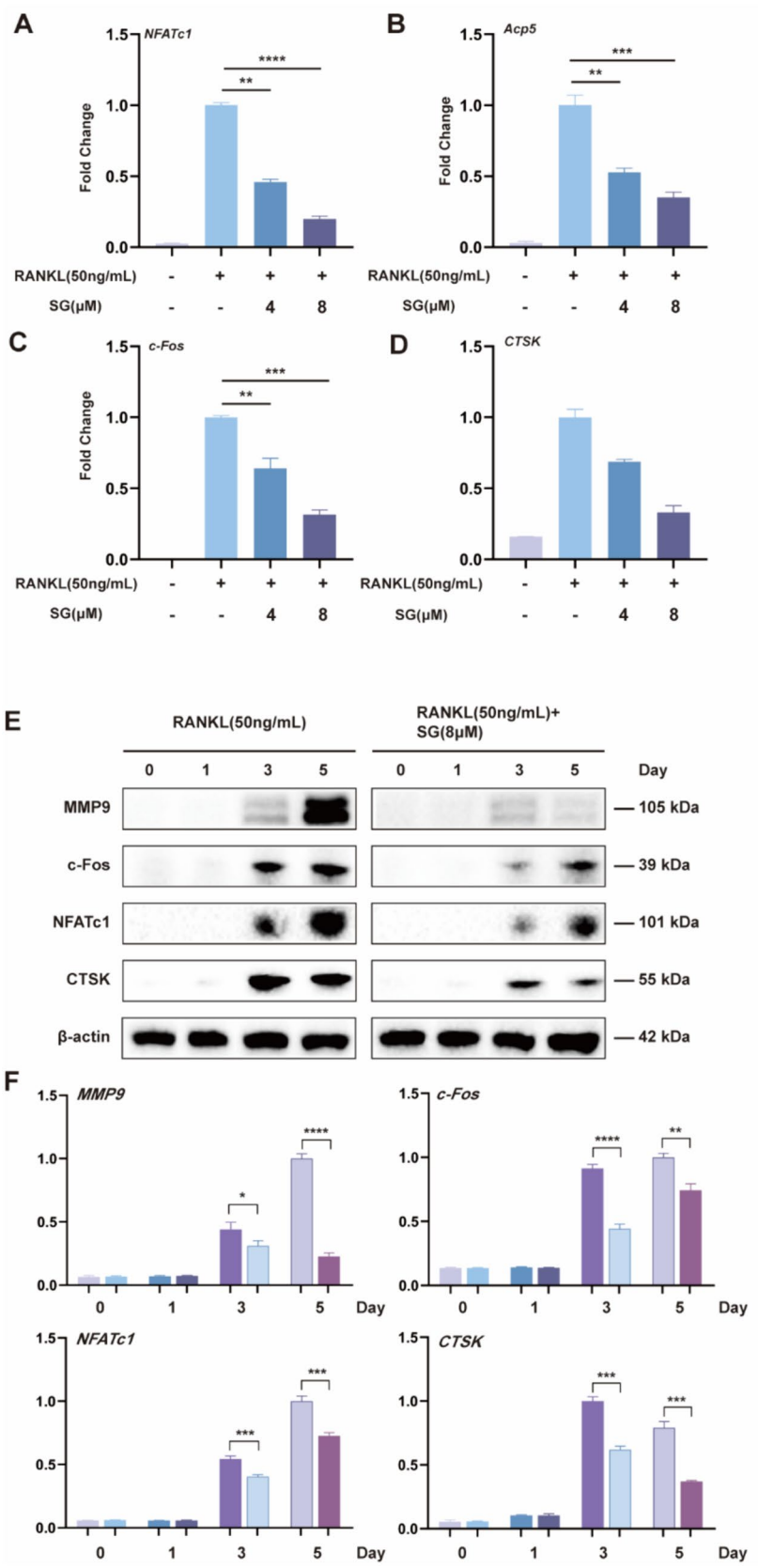

Fig. 2 Sophoraflavanone G (SG) can suppress the relative expression of genes and proteins specific to OC differentiation, and as the concentration increases, the inhibitory effect becomes more evident. **A**, **B**, **C**, **D**: As the concentration increases, the inhibitory effect of SG on the expression of OC differentiation-related genes becomes stronger; **E**: Under RANKL stimulation, the relative expression levels of MMP9, NFATc1, CTSK, and c-Fos increase steadily, with MMP9, c-Fos, and NFATc1 peaking on day 5. However, under SG influence, they show a declining trend, with significant statistical differences observed on days 3 and 5. CTSK is expressed highest on day 3, where SG's inhibitory effect is most evident; **F**: Bar chart analysis of proteins specific to OC differentiation. $*p<0.05$, $**p<0.01$, $***p<0.001$ ($n=3$)

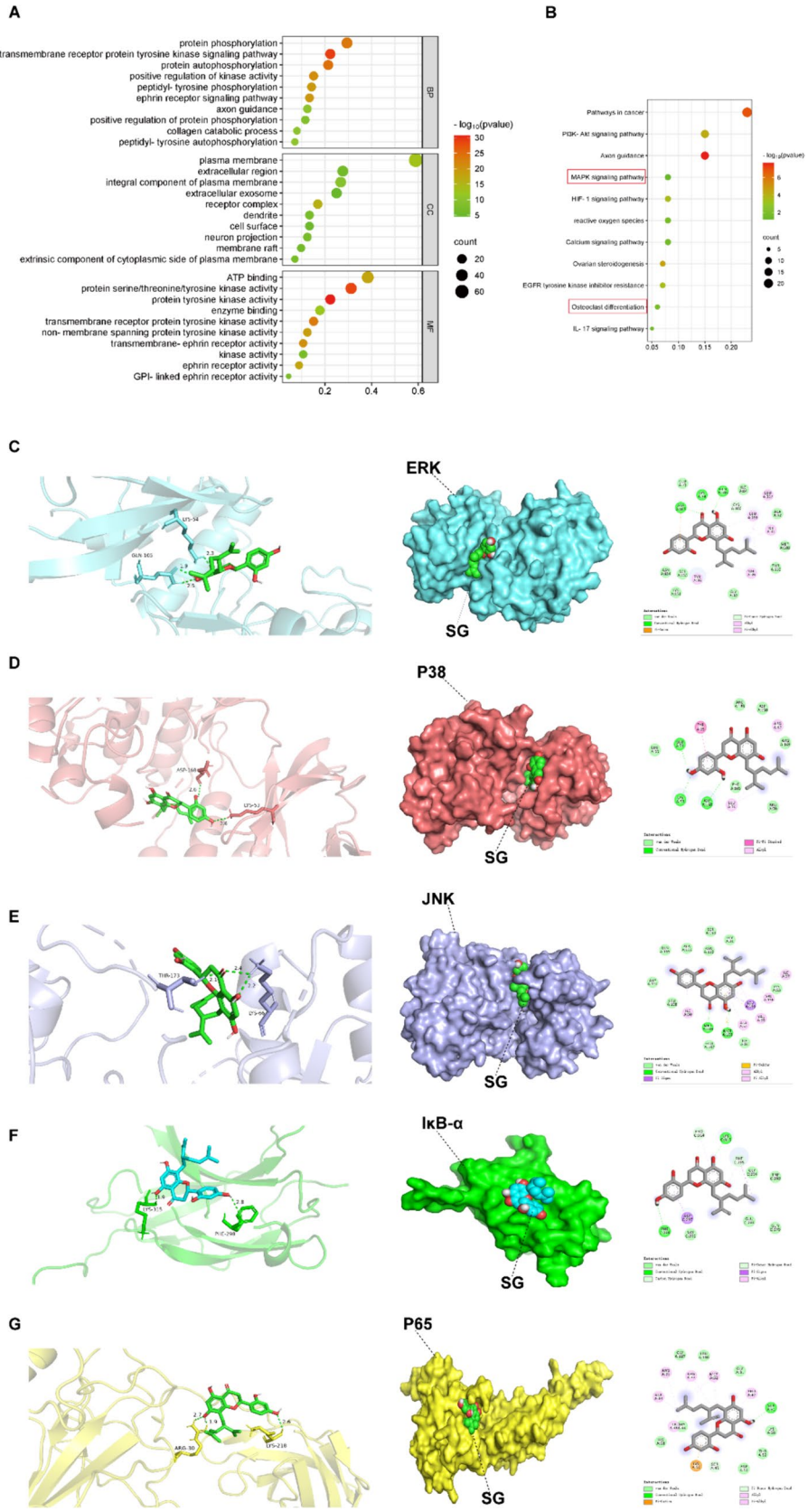

Fig. 3 GO and KEGG analysis results and molecular docking diagrams. **A**: GO analysis of related biological functions; **B**: KEGG analysis of related signaling pathways; **C**, **D**, **E**, **F**, **G**: 3D and 2D schematic diagrams of SG docked with ERK, P38, JNK, IκB-α, and P65

activity. KEGG analysis identified signaling pathways closely related to OC differentiation, including MAPK, PI3K-AKT, HIF-1, calcium ions, EGFR, and IL-17 (Fig. 3B). Molecular docking results showed that SG binds with high affinity to ERK, JNK, P38, P65, and IκB-α, with JNK and ERK having the highest binding affinities. We visualized these results using the AutoDock software; Figs. 3C, D, E, F, G, respectively, illustrate the 3D and 2D docking structures and visual docking of SG with target proteins.

SG Inhibits OC Formation via the MAPK/NF-κB Pathway

The MAPK/NF-κB pathway plays a crucial role in regulating OC differentiation and has been extensively studied due to its vital involvement in OP prevention.

The results in Fig. 4A highlight that IGG can effectively reduce the phosphorylated expression level of JNK at 15 and 30 min. Simultaneously, at 15, 30, 45, and 60 min, SG consistently shows the significant inhibitory trend in the phosphorylated expression level of ERK. Notably, at the 30, 45, and 60-min marks, there is an evident increased trend in the phosphorylated expression of P38 compared to the positive control group (Fig. 4B, C, D). Similarly, as shown in Fig. 4E, regarding the NF-κB pathway, SG can inhibit the phosphorylated expression level of P65 at 15 min, but this effect disappears by the 60-min mark. As for IκB-α, SG fails to prevent its degradation (Fig. 4F, G).

SG Reduces Bone Loss

To further validate the in *vitro* experiments, we intervened with different animal groups, establishing an osteoporotic mouse model and administering intraperitoneal injections. Interventions on the rat model with drugs or saline lasted for a total of 8–10 weeks. Using Micro-CT technology, we obtained significant results: SG effectively alleviated OP caused by heightened OC activity. Compared to the sham surgery group (Sham), the osteoporotic group (OP) exhibited a notable reduction in the number of trabecular bones and a significant decrease in bone density (Fig. 5A). However, in the SG group, these phenomena were significantly mitigated, with both bone density and trabecular bone thickness showing increases. The degree of separation of trabecular bones compared to the osteoporotic (OP) group showed a significant decline (Fig. 5B).

Discussion

OP, as the most prevalent metabolic bone disease globally, leads to severe complications such as fragility fractures, ambulatory difficulties, deformities, pain, and high rates of disability and mortality, significantly diminishing patients' quality of life and healing outcomes [27]. Common medications used in the clinical treatment of OP include Bisphosphonates, Denosumab, Teriparatide, Selective estrogen receptor Modulators, and Vitamin D. These treatments have garnered widespread recognition and validation for their efficacy, achieving substantial success. However, the side effects associated with these medications can sometimes constrain their clinical application [28].

Traditional Chinese Medicine has a venerable history in treating skeletal disorders and has increasingly gained attention for its widespread clinical use and satisfactory therapeutic outcomes, having long been employed in the management of OP. The core mechanism of Traditional Chinese Medicine in treating OP involves promoting the differentiation of OB to increase bone mass and inhibiting the formation of OC to reduce bone resorption activity. Consequently, the urgent quest to leverage the therapeutic effects of traditional Chinese medicine to discover a cost-effective and efficient treatment for osteoporosis is paramount. Herein, we have demonstrated that SG, at lower concentrations, can mitigate OC differentiation via *the* MAPK/NF-κB signaling pathway, alleviating bone loss induced by OC. These findings not only provide a scientific basis for the clinical use of SG in the treatment of OP but also highlight the potential advantages of Traditional Chinese Medicine in regulating bone remodeling.

This investigation initially ascertained the effective concentration of SG in inhibiting OC differentiation through CCK-8 and TRAP staining, demonstrating that SG primarily targets OC, thereby facilitating the bone remodeling process to treat OP.

The process of bone remodeling is primarily participated in by OB and OC. The interaction between OB and OC is fundamental for bone growth, development, repair, and regeneration. The interaction of OC with a resorptive function in bone tissue, regulated by the immune system's monocyte-macrophage lineage, and OB, which predominantly promotes skeletal structural development, is crucial for maintaining a dynamic equilibrium in bones and the ongoing bone remodeling process.

Bone remodeling typically involves four phases: (1) Recruitment of OC to the bone surface and its activation; (2) The phase where mature OC performs bone resorption; (3) Recruitment of progenitor OB to the pit after OC death; (4) Mature OB producing bone tissue to fill the gap [29]. The dynamic balance between bone formation mediated by OB and bone resorption by OC remains relatively unchanged under stable conditions, ultimately, maintaining a healthy skeletal system.

We also explored the impact of SG on the relative expression levels of specific genes and proteins during the maturation process of OC formation, including

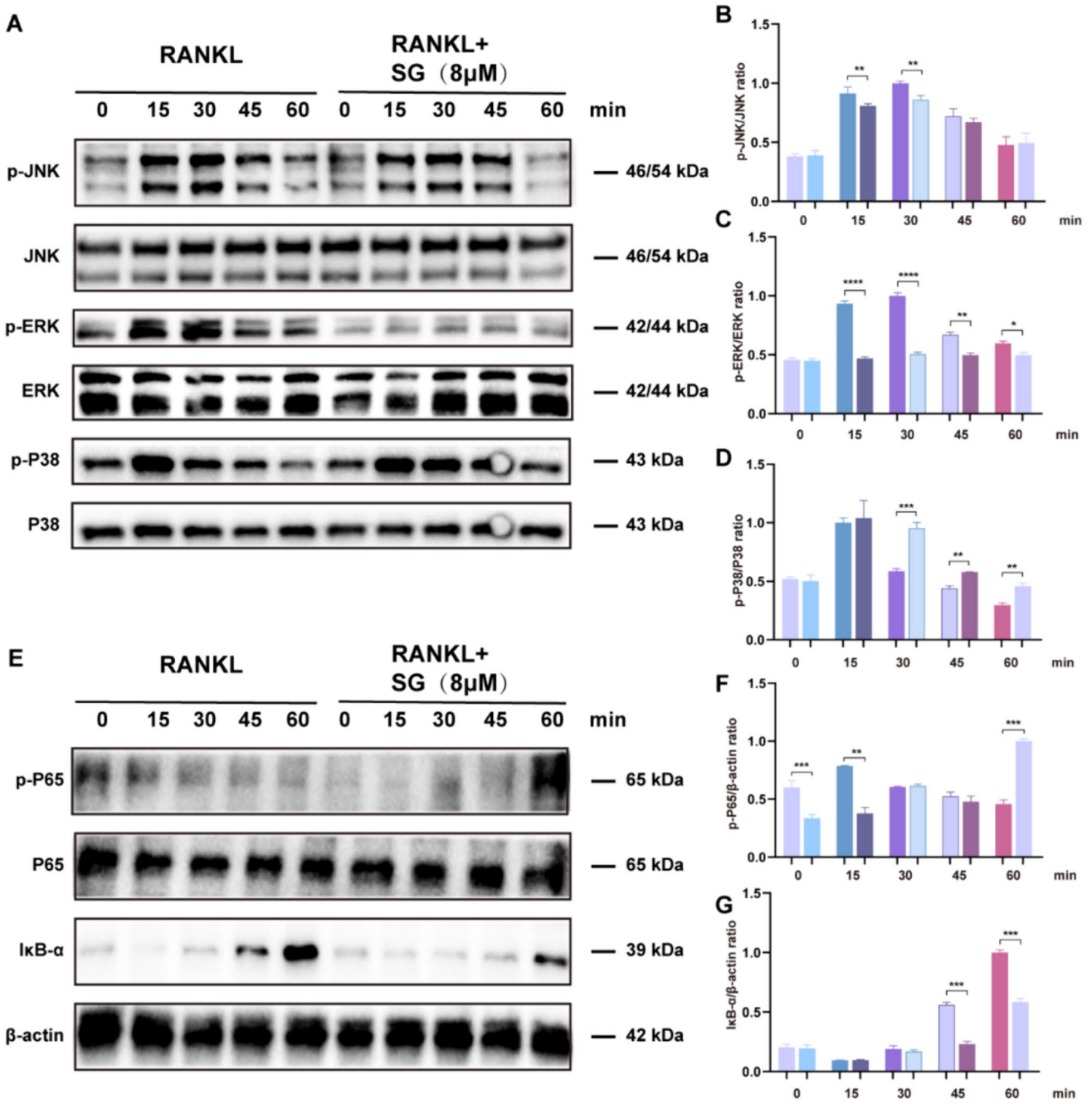

Fig. 4 Sophoraflavanone G (SG) affects the phosphorylated expression of proteins in the MAPK/NF-κB pathway. **A**, **B**, **C**, **D**: IGG demonstrates varying inhibitory effects on the phosphorylated expression of ERK and JNK proteins in MAPK at different time points, with each time point having its distinct characteristics. However, there is no significant inhibitory effect on the phosphorylation of P38. **E**, **F**: SG fails to inhibit the phosphorylated expression of P65 and cannot prevent the degradation of IκB-α

NFATc1, c-Fos, MMP9, and CTSK. These genes and proteins exert significant influence over the proliferation, survival, maturation, and differentiation processes of OC. The NFATc1, as the pivotal transcription factor in OC differentiation, is controlled by the RANK-RANKL axis. It activates the TRAF6, leading to NFATc1 transcribing into the cell nucleus, promoting the expression of OC differentiation-specific proteins such as CTSK, c-Fos, and MMP9 [30, 31]. Notably, when NFATc1 is suppressed or knocked out, bone marrow-derived embryonic stem cells can't differentiate into mature OC [32, 33].

CTSK, as the cysteine protease belonging to the papain family, emerges during the early stages of OC differentiation [34].CTSK is a key member downstream of NFATc1 genes

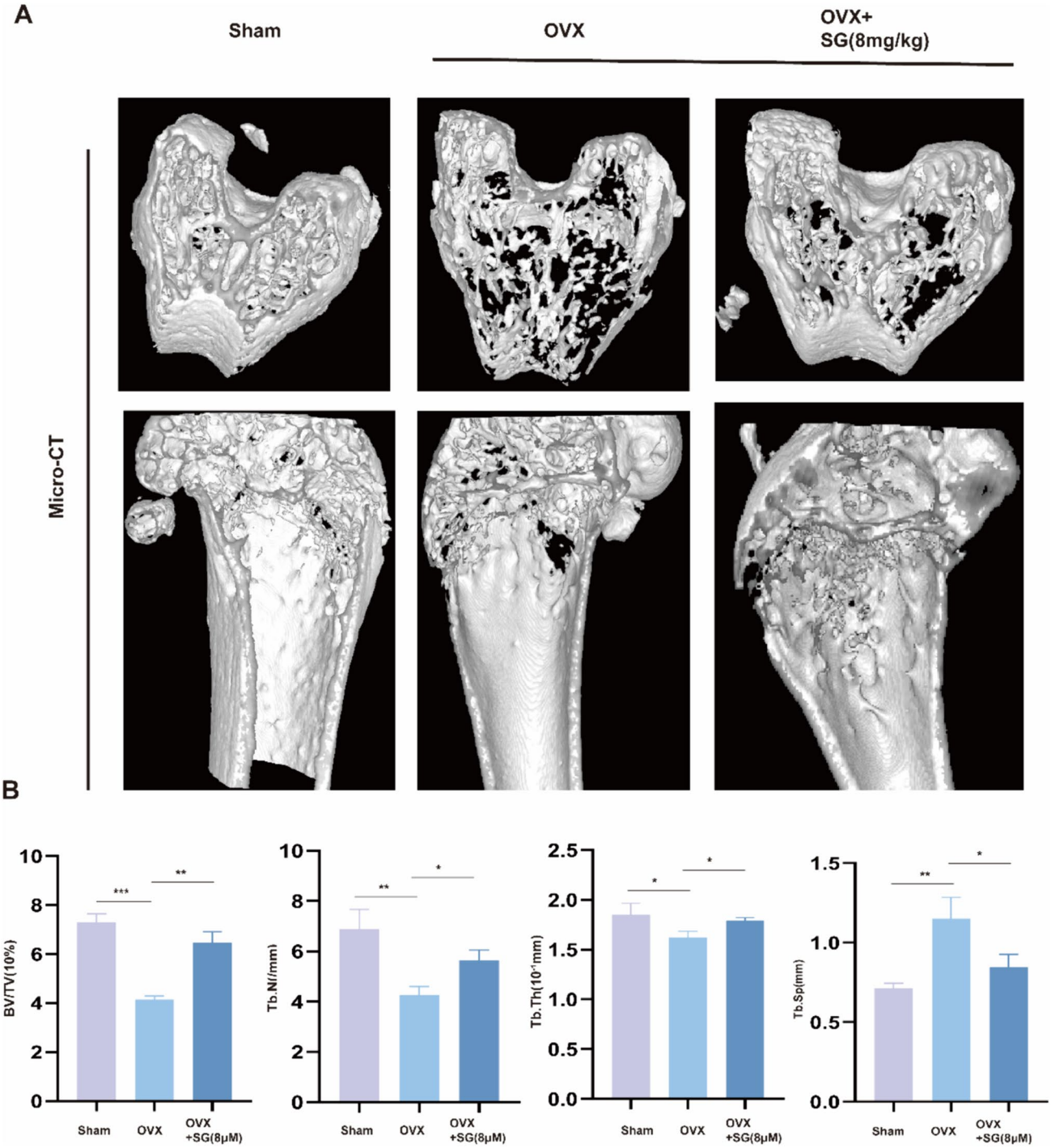

Fig. 5 Sophoraflavanone G (SG) ameliorates bone loss. **A**: Compared to the sham surgery group (Sham), the osteoporotic group (OP) shows a significant reduction in bone mass, but this loss is notably alleviated after SG stimulation; **B**: Column charts analyzing data related to the number and thickness of trabecular bones. $*p<0.05$, $**p<0.01$, $***p<0.001$ ($n=6$)

and an important epigenetic regulator, and it plays the pivotal role during bone resorption, also participating in regulating OC apoptosis and aging processes [35, 36].

Our findings suggest that SG is capable of suppressing the expression levels of these genes and proteins, thereby affecting the formation of mature OC and bone resorption activity, which contributes to the amelioration of bone mass reduction.

Our research also unveils that SG plays the role in modulating the MAPK/NF-κB pathway under the

stimulation of RANKL, which is indispensable in the differentiation of OC.

The MAPK family serves as connectors for extracellular stimuli, converting external stimuli into specific cellular responses [37, 38]. Extracellular stimuli regulate OC differentiation and bone remodeling process by activating MAPK, where ERK, JNK, and P38 are significant regulators [39]. The ERK signaling pathway positively regulates various biological activities in osteoclasts, such as proliferation, differentiation, and apoptosis. When ERK is knocked out or silenced, the number of OC progenitor cells decreases, inhibiting the OC fusion phenotype stimulated by M-CSF, and bone mineral density increases [40]. Accompanied by M-CSF induction, downstream transcription factors of ERK like c-Fos and NFATc1 are also activated, regulating osteoclast formation [41, 42].JNK is closely related to apoptosis during OC differentiation and regulates the activity of bone resorption [43, 44].

When JNK's activity or expression is blocked, the process of osteoclast multinucleation stops, even reverting from a multinucleated morphology back to a monocyte form [39, 45].P38 plays a leading role in mature osteoclast differentiation, regulating bone resorption activity and bone remodeling. When P38's expression or activity is inhibited, $P38^{-/-}$ mouse models show a noticeable increase in bone mass, a decrease in OC-led bone resorption activity, and the reduction in their number [46, 47].

Under the impetus of RANKL and TNFα, TRAF6 enlists proteins such as IKK-α and IKK-β from the receptor-activated NF-κB signaling pathway. This provokes the degradation of IκB-α and the emancipation of the P65/P50 complex, directing the nuclear translocation of P65 and thereby stimulating the expression of target genes associated with mature OC [31]. However, our experimental findings suggest that, initially, IGG can inhibit the level of phosphorylated P65 expression, this influence wanes by the 60th-minute mark. As for IκB-α, IGG was unable to resuscitate the protein's degradation, indicating that IGG has not shown significant trends in affecting the proteins in the NF-κB signaling pathway.

In summary, our research outcomes align with established literature findings [24]: SG manifests commendable binding affinity with CTSK. In vitro experiments illustrate that IGG can inhibit OC formation and impact the expression levels of pertinent genes and proteins at low concentrations. We have also discovered that SG can suppress ERK, JNK, and P65 signal transduction pathways in MAPK and NF-κB, thereby achieving the goal of osteoporosis resistance. Animal experiments confirm the reliability of in *vitro* tests and prove in *vivo* that SG can reduce OC formation, rescue bone loss, and potentially treat OP.

However, the anti-inflammatory function has yet to be substantiated in this study. Beyond OC, it remains unaffirmed whether IGG can ameliorate inflammation and thereby reduce bone loss while promoting OB differentiation and bone formation. Nonetheless, these insights motivate me to continue further research in this direction in the future.

Acknowledgements None.

Author Contributions XC L, W D, and K T prepared and revised the manuscript and made equal contributions to this paper. SY Z, WW L, and ZX L performed qPCR and Western Blot. YY L and SM C participated in animal experiments. XC L, W D, and K T prepared the figures and legends. ZD Z, WH Z, and J Z designed and supervised the overall study and revised the manuscript.

Funding Plan on enhancing scientific research in GMU, Guangzhou, China (2023); The Science and Technology Project of Guangzhou(Number:2023A04J1856,2023A03J0779); College Students' Innovation and Entrepreneurship Competition of Guangzhou University of Chinese Medicine(Number:202210572184); Project supported by Hainan Province Clinical Medical Center([2021] No. 276). Dongguan Social Development Technology Project (20231800940022).

Data Availability Source materials and literature will be provided as needed.

Declarations

Ethical Approval Animal experiments were adopted by the Guangzhou University of Chinese Medicine Animal Ethics Committee (Number: 20231009001).

References

1. Czerwinski, E. (1994). Diagnosis of osteoporosis. *Przeglad Lekarski, 51*, 391–397.
2. Salari, N., et al. (2021). The global prevalence of osteoporosis in the world: A comprehensive systematic review and meta-analysis. *Journal of Orthopaedic Surgery and Research, 16*, 609. https://doi.org/10.1186/s13018-021-02772-0
3. Gregson, C. L., et al. (2022). UK clinical guideline for the prevention and treatment of osteoporosis. *Archives of Osteoporosis, 17*, 58. https://doi.org/10.1007/s11657-022-01061-5
4. Marcucci, G., & Brandi, M. L. (2015). Rare causes of osteoporosis. *Clinical Cases in Mineral and Bone Metabolism, 12*, 151–156. https://doi.org/10.11138/ccmbm/2015.12.2.151
5. Kanis, J. A., et al. (2021). SCOPE 2021: A new scorecard for osteoporosis in Europe. *Archives of Osteoporosis, 16*, 82. https://doi.org/10.1007/s11657-020-00871-9
6. Rosen, C. J (2000). in *Endotext* (eds K. R. Feingold *et al.*).
7. Neve, A., Corrado, A., & Cantatore, F. P. (2011). Osteoblast physiology in normal and pathological conditions. *Cell and Tissue Research, 343*, 289–302. https://doi.org/10.1007/s00441-010-1086-1
8. Berardi, S., Corrado, A., Maruotti, N., Cici, D., & Cantatore, F. P. (2021). Osteoblast role in the pathogenesis of rheumatoid arthritis. *Molecular Biology Reports, 48*, 2843–2852. https://doi.org/10.1007/s11033-021-06288-y
9. Ono, T., & Nakashima, T. (2018). Recent advances in osteoclast biology. *Histochemistry and Cell Biology, 149*, 325–341. https://doi.org/10.1007/s00418-018-1636-2
10. Soe, K. (2020). Osteoclast fusion: Physiological regulation of multinucleation through heterogeneity-potential implications for

drug sensitivity. *International Journal of Molecular Sciences, 21*(20), 7717.
11. Brom, V. C., et al. (2023). Agonistic and antagonistic targeting of immune checkpoint molecules differentially regulate osteoclastogenesis. *Frontiers in Immunology, 14*, 988365. https://doi.org/10.3389/fimmu.2023.988365
12. Hua, R., Gu, S., & Jiang, J. X. (2022). Connexin 43 hemichannels regulate osteoblast to osteocyte differentiation. *Frontiers in Cell and Developmental Biology, 10*, 892229. https://doi.org/10.3389/fcell.2022.892229
13. McClung, M., et al. (2013). Bisphosphonate therapy for osteoporosis: Benefits, risks, and drug holiday. *American Journal of Medicine, 126*, 13–20. https://doi.org/10.1016/j.amjmed.2012.06.023
14. Gehrke, B., Alves Coelho, M. C., Brasil d'Alva, C., & Madeira, M. (2023). Long-term consequences of osteoporosis therapy with bisphosphonates. *Archives of Endocrinology Metabolism, 68*, e220334. https://doi.org/10.20945/2359-4292-2022-0334
15. Bellido, T. (2024). Bisphosphonates for osteoporosis: from bench to clinic. *The Journal of Clinical Investigation*. https://doi.org/10.1172/JCI179942
16. Ferrari-Lacraz, S., & Ferrari, S. (2011). Do RANKL inhibitors (denosumab) affect inflammation and immunity? *Osteoporosis International, 22*, 435–446. https://doi.org/10.1007/s00198-010-1326-y
17. Kendler, D. L., Cosman, F., Stad, R. K., & Ferrari, S. (2022). Denosumab in the treatment of osteoporosis: 10 years later: A narrative review. *Advances in Therapy, 39*, 58–74. https://doi.org/10.1007/s12325-021-01936-y
18. McDonald, M. M., Kim, A. S., Mulholland, B. S., & Rauner, M. (2021). New insights into osteoclast biology. *Journal of Bone and Mineral Research Plus, 5*, e10539. https://doi.org/10.1002/jbm4.10539
19. Kim, B. H., et al. (2013). Sophoraflavanone G induces apoptosis of human cancer cells by targeting upstream signals of STATs. *Biochemical Pharmacology, 86*, 950–959. https://doi.org/10.1016/j.bcp.2013.08.009
20. Cheng, W., Liu, D., Guo, M., Li, H., & Wang, Q. (2022). Sophoraflavanone G suppresses the progression of triple-negative breast cancer via the inactivation of EGFR-PI3K-AKT signaling. *Drug Development Research, 83*, 1138–1151. https://doi.org/10.1002/ddr.21938
21. Wang, H., Tong, Y., Xiao, D., & Xia, B. (2020). Involvement of mTOR-related signaling in antidepressant effects of Sophoraflavanone G on chronically stressed mice. *Phytotherapy Research, 34*, 2246–2257. https://doi.org/10.1002/ptr.6675
22. Wang, M. C., et al. (2022). Sophoraflavanone G from *Sophora flavescens* ameliorates allergic airway inflammation by suppressing Th2 response and oxidative stress in a murine asthma model. *International Journal of Molecular Sciences*. https://doi.org/10.3390/ijms23116104
23. Yang, Z., et al. (2019). Solid self-microemulsifying drug delivery system of Sophoraflavanone G: Prescription optimization and pharmacokinetic evaluation. *European Journal of Pharmaceutical Sciences, 136*, 104953. https://doi.org/10.1016/j.ejps.2019.06.007
24. Qiu, Z. C., et al. (2016). Discovery of a new class of Cathepsin K inhibitors in rhizoma drynariae as potential candidates for the treatment of osteoporosis. *International Journal of Molecular Sciences*. https://doi.org/10.3390/ijms17122116
25. Deng, W., et al. (2022). Dehydromiltirone inhibits osteoclast differentiation in RAW2647 and bone marrow macrophages by modulating MAPK and NF-kappaB activity. *Frontiers in Pharmacology*. https://doi.org/10.3389/fphar.2022.1015693
26. Liu, Y. D., Liu, J. F., & Liu, B. (2022). N, N-Dimethylformamide inhibits high glucose-induced osteoporosis via attenuating MAPK and NF-kappaB signalling. *Bone Joint Research, 11*, 200–209. https://doi.org/10.1302/2046-3758.114.BJR-2020-0308.R2
27. Handel, M. N., et al. (2023). Fracture risk reduction and safety by osteoporosis treatment compared with placebo or active comparator in postmenopausal women: Systematic review, network meta-analysis, and meta-regression analysis of randomised clinical trials. *BMJ, 381*, e068033. https://doi.org/10.1136/bmj-2021-068033
28. Kanis, J. A., et al. (2019). European guidance for the diagnosis and management of osteoporosis in postmenopausal women. *Osteoporosis International, 30*, 3–44. https://doi.org/10.1007/s00198-018-4704-5
29. Kim, J. M., Lin, C., Stavre, Z., Greenblatt, M. B., & Shim, J. H. (2020). Osteoblast-osteoclast communication and bone homeostasis. *Cells*. https://doi.org/10.3390/cells9092073
30. Paramasivam, S., & Perumal, S. S. (2023). Methanolic extract of *O.umbellata* L. exhibits anti-osteoporotic effect via promoting osteoblast proliferation in MG-63 cells and inhibiting osteoclastogenesis in RANKL-stimulated RAW 264.7 cells. *Journal of Ethnopharmacology, 315*, 116641. https://doi.org/10.1016/j.jep.2023.116641
31. Yao, Z., Getting, S. J., & Locke, I. C. (2021). Regulation of TNF-induced osteoclast differentiation. *Cells*. https://doi.org/10.3390/cells11010132
32. Chen, S., et al. (2023). Macrophages in immunoregulation and therapeutics. *Signal Transduction and Targeted Therapy, 8*, 207. https://doi.org/10.1038/s41392-023-01452-1
33. Fujioka, S., et al. (2004). NF-kappaB and AP-1 connection: Mechanism of NF-kappaB-dependent regulation of AP-1 activity. *Molecular and Cellular Biology, 24*, 7806–7819. https://doi.org/10.1128/MCB.24.17.7806-7819.2004
34. Zou, N., Liu, R., & Li, C. (2022). Cathepsin K(+) Non-osteoclast cells in the skeletal system: Function, models, identity, and therapeutic implications. *Frontiers in Cell and Developmental Biology, 10*, 818462. https://doi.org/10.3389/fcell.2022.818462
35. Lotinun, S., et al. (2013). Osteoclast-specific cathepsin K deletion stimulates S1P-dependent bone formation. *The Journal of Clinical Investigation, 123*, 666–681. https://doi.org/10.1172/JCI64840
36. Xin, Y., et al. (2020). New function of RUNX2 in regulating osteoclast differentiation via the AKT/NFATc1/CTSK axis. *Calcified Tissue International, 106*, 553–566. https://doi.org/10.1007/s00223-020-00666-7
37. Chang, L., & Karin, M. (2001). Mammalian MAP kinase signalling cascades. *Nature, 410*, 37–40. https://doi.org/10.1038/35065000
38. Dong, W., et al. (2022). Myocardin-related transcription factor A drives ROS-fueled expansion of hepatic stellate cells by regulating p38-MAPK signalling. *Clinical and Translational Medicine, 12*, e688. https://doi.org/10.1002/ctm2.688
39. Lee, K., Seo, I., Choi, M. H., & Jeong, D. (2018). Roles of mitogen-activated protein kinases in osteoclast biology. *International Journal of Molecular Science*. https://doi.org/10.3390/ijms19103004
40. He, Y., et al. (2011). Erk1 positively regulates osteoclast differentiation and bone resorptive activity. *PLoS ONE, 6*, e24780. https://doi.org/10.1371/journal.pone.0024780
41. Lee, M. S., et al. (2009). GM-CSF regulates fusion of mononuclear osteoclasts into bone-resorbing osteoclasts by activating the Ras/ERK pathway. *The Journal of Immunology, 183*(5), 3390–3399.
42. Weilbaecher, K. N., et al. (2001). Linkage of M-CSF signaling to Mitf, TFE3, and the osteoclast defect in Mitf(mi/mi) mice. *Molecular Cell, 8*, 749–758. https://doi.org/10.1016/s1097-2765(01)00360-4
43. David, J. P., Sabapathy, K., Hoffmann, O., Idarraga, M. H., & Wagner, E. F. (2002). JNK1 modulates osteoclastogenesis through both c-Jun phosphorylation-dependent and-independent

mechanisms. *Journal of Cell Science, 115*, 4317–4325. https://doi.org/10.1242/jcs.00082
44. Ikeda, F., et al. (2008). JNK/c-Jun signaling mediates an anti-apoptotic effect of RANKL in osteoclasts. *Journal of Bone and Mineral Research, 23*, 907–914. https://doi.org/10.1359/jbmr.080211
45. Chang, E. J., et al. (2008). The JNK-dependent CaMK pathway restrains the reversion of committed cells during osteoclast differentiation. *Journal of Cell Science, 121*, 2555–2564. https://doi.org/10.1242/jcs.028217
46. Cong, Q., et al. (2017). p38alpha MAPK regulates proliferation and differentiation of osteoclast progenitors and bone remodeling in an aging-dependent manner. *Science and Reports, 7*, 45964. https://doi.org/10.1038/srep45964
47. Matsumoto, M., Sudo, T., Saito, T., Osada, H., & Tsujimoto, M. (2000). Involvement of p38 mitogen-activated protein kinase signaling pathway in osteoclastogenesis mediated by receptor activator of NF-kappa B ligand (RANKL). *Journal of Biological Chemistry, 275*, 31155–31161. https://doi.org/10.1074/jbc.M001229200